Eur Radiol (2007) 17: 2359–2367
DOI 10.1007/s00330-007-0632-z

PHYSICS

John Stratakis
John Damilakis
Dimitrios Tsetis
Nicholas Gourtsoyiannis

Radiation dose and risk from fluoroscopically guided percutaneous transluminal angioplasty and stenting in the abdominal region

Received: 14 June 2006
Revised: 18 February 2007
Accepted: 9 March 2007
Published online: 27 March 2007

J. Stratakis · J. Damilakis (✉)
Department of Medical Physics,
University of Crete,
P.O. Box 2208,
Iraklion, Crete, 71003, Greece
e-mail: damilaki@med.uoc.gr
Tel.: +30-2810-392569
Fax: +30-2810-542095

D. Tsetis · N. Gourtsoyiannis
Department of Radiology,
University of Crete,
P.O. Box 2208,
Iraklion, Crete, 71003, Greece

Abstract The objective of this study was to estimate the radiation dose and associated risks resulting from fluoroscopically guided percutaneous transluminal angioplasty with or without stent placement in the abdominal region. Average examination parameters for renal and aortoiliac procedures were derived using data from 80 consecutive procedures performed in our institute. Organ and effective doses were estimated for endovascular procedures with the use of a Monte Carlo (MC) transport code and an adult mathematical phantom. Thermoluminescent dosimeters were used in an anthropomorphic phantom to verify MC calculations. Radiation-induced risks were estimated. Results are presented as doses normalized to dose area product, so that the patient dose from any technique and X-ray unit can be easily calculated for iliac and renal PTA/stenting sessions. The average effective dose varied from 75 to 371 μSv per Gycm^2 depending on the beam quality, procedure scheme and sex of the patient. Differences up to 17% were observed between MC-calculated data and data derived from thermoluminescent dosimetry. The radiation-induced cancer risk may be considerable for younger individuals undergoing transluminal angioplasty with stent placement.

Keywords Radiation dosimetry · Percutaneous transluminal angioplasty · Stent placement · Radiation risks · Normalized effective dose · Monte Carlo simulation

Introduction

Percutaneous transluminal angioplasty (PTA) with elective stenting is an established treatment method for an increasing number of patients with peripheral and renovascular atherosclerotic stenotic and occlusive disease (AOD) [1, 2]. The aorta and iliac arteries have become a widely accepted field for percutaneous interventions because of the easy access to the lesions, the relatively large diameter of the target vessels and the comparably benign outcome even of major complications [3]. In addition, endovascular treatment has replaced surgical revascularization for most patients with renal artery stenosis (RAS) resulting from atherosclerotic and fibromuscular disease who meet the criteria for intervention [4, 5].

Prolonged fluoroscopy times are frequently observed in complex endovascular procedures even when performed by experienced operators with the use of dose-reducing technology and modern fluoroscopic equipment [6–11]. National and regional authorized bodies have recently pointed out the increasing number of IR procedures and recommended monitoring and recording of patient dose data for quality assurance purposes as well as for patient safety [12–14].

Among other methods [15–17], Monte Carlo (MC) techniques have been employed to simulate radiation transport in the human body and produce normalized patient dose data [18–20]. Normalized dosimetric data incorporate a major advantage in comparison with surface or air kerma measurements, since the effective dose from

an IR procedure can be estimated by multiplying the total DAP of the procedure with a conversion coefficient. To our knowledge there are no normalized patient dose data in the literature associated with renal and iliac endovascular IR procedures.

The aim of the current study was to (1) provide normalized to DAP organ and effective dose data associated with renal and iliac endovascular procedures and (2) estimate radiation doses and risks related to typical renal and iliac endovascular procedures.

Materials and methods

Fluoroscopy equipment

A floor-mounted Siemens Axiom Artis digital angiographic system (Siemens, Enlargen, Germany) was used in the current study. The tube housing incorporated a high-output, liquid-cooled, three-foci X-ray tube, a 12° anode angle and a total filtration of 5.5 mm Al equivalent. An image intensifier of a nominal circular field size of 40 cm was used. Tube potential and current were altered through automatic exposure control. The radiation dose in terms of DAP and cumulative dose (CD) was monitored by an ionization chamber incorporated in the collimation system. CD is the air kerma accumulated at a specific point in space along the central ray, 15 cm from the fluoroscopy system's isocenter in the direction of the focal spot, usually defined as the interventional reference point (IRP) [21].

Patient population

In the current study, 80 consecutive patients suffering from RAS or AOD were treated with percutaneous endovascular procedures in our IR laboratory. This study was carried out in accordance with Helsinki Declaration, and written consent was obtained from all patients. Patients were separated into two groups: group A consisted of 24 subjects on whom renal artery revascularization was undertaken, and group B comprised 56 subjects treated percutaneously for iliac stenosis or occlusion. Indications for renal artery revascularization included patients with difficult-to-control hypertension and/or deterioration in renal function and an angiographic diameter stenosis greater than 50% in combination with a translesional systolic pressure gradient ≥15 mmHg. Indications for aortoiliac PTA/stenting included patients with disabling claudication or critical limb ischemia and angiographically documented TASC A, B as well as selective TASC C lesions in patients considered as poor surgical candidates [22]. All interventions were performed by the same experienced interventional radiologist (DT). Pulsed fluoroscopy of 15 pulses per second, with a pulse width of 25 ms, was used.

The most commonly used vascular access for revascularization of the common iliac artery (CIA) and external iliac artery (EIA) was retrograde common femoral artery (CFA) access. When the very distal portion of the EIA was involved, contralateral access was preferred. A baseline angiogram was then obtained with hand injection of contrast through the sheath, followed in the majority of cases by a 20-degree contralateral oblique projection in order to separate the origin of the internal and external iliac arteries. After crossing the lesion by a 0.035″ soft tip or hydrophilic guidewire alone or in combination with a supportive diagnostic catheter, this wire was exchanged for a 0.035″ extra-stiff guidewire (Amplatz wire, Cook Inc, Bloomington, IN) to provide support and trackability for balloon and/or stent placement. Aortic bifurcational lesions were treated with simultaneous predilation and subsequent stent deployment through a bilateral retrograde approach (Kissing technique).

For RAS endovascular treatment, a 6F 35–40-cm-long sheath was inserted through retrograde CFA access and its tip was placed in close proximity with the ostium of the renal artery. Posterior-anterior (PA) and 20-degree left anterior oblique angiographic projections were used for optimal lesion visualization. Catheterization of the renal artery was performed by a 5F diagnostic catheter (Sidewinder or Cobra) and a steerable 0.014″ or 0.018″ guidewire with a flexible tip. After crossing the lesion the diagnostic catheter was exchanged for the balloon or stent-delivery catheter.

Primary stent placement was considered in total occlusions, complex stenoses (i.e, long irregularly surfaced stenoses, markedly ulcerated plaques, plaques with heavy calcification, severely eccentric plaques and plaques with spontaneous dissection), CIA lesions with extension to the aortic bifurcation and renal ostial lesions. The rest of the stenoses underwent first PTA with a balloon of the same size as the target vessel and elective stent placement in case of: (1) a residual stenosis greater than 30%, (2) an obstructive dissection, (3) a residual resting mean transstenotic pressure gradient >10 mmHg and (4) a combination of the above. A conclusion angiogram was obtained in all cases to verify the result of the endovascular procedure. Technical and physical parameters for fluoroscopy, digital radiography and digital subtraction angiography (DSA) were recorded. The tube voltage, tube load, fluoroscopy time and number of radiographic exposures were recorded during the IR procedure. The total DAP for each IR procedure and separate DAP contributions corresponding to fluoroscopy and DSA were measured using the integrated DAP meter of the fluoroscopy system. The estimation of CD values was based on air kerma measurements at the IRP. The number of frames was retrospectively recorded from the X-ray machine console at the end of each procedure. Patient data were utilized to determine average examination parameters for renal and iliac angioplasty procedures.

Monte Carlo simulation

The Monte-Carlo-N-particle (MCNP4C2, Los Alamos National Laboratory, Los Alamos, NM) code system was employed to simulate dose deposition in the human body [23]. The user-supplied input file contained information about the X-ray source specification and the geometry of the IR procedure in terms of beam angle, source to patient distance and field size. Human anatomy was replicated by an hermaphroditic mathematical phantom constructed with BodyBuilder (White Rock Science NM), representing an adult human body of 1.75 m in height and 71 kg in weight (BMI=23.2 kg/m^2). Composition of the human body was modeled by assigning skeletal, soft or lung material to corresponding tissues [24]. Monte Carlo simulations were performed for tube voltages ranging from 70 to 90 kVp. Diagnostic energy spectra developed by Nowotny [25] were used in the MCNP input file. Siemens CAREFILTER was simulated by adding 0.0 to 0.9 mm of copper in the useful beam.

Organ doses were calculated for an adult phantom simulating patients undergoing PTA in the renal and iliac arteries. Energy deposition was recorded for commonly used PA, 20° left anterior oblique and 20° right anterior oblique projections, as instructed by the interventional radiologist. Energy deposition in each of the modeled organs was calculated using f5 and f6 tally scoring. Tallies are mathematical detectors used in MCNP simulations. Organ doses were divided with total DAP to provide DAP to organ dose conversion factors for each projection.

Effective dose calculations normalized to DAP were performed according to the International Commission on Radiological Protection (ICRP) recommendations [26]. The dose to the bone surface was taken to be the dose to the skeleton, that is, the sum of normalized doses for cells incorporating bone density in the phantom [24]. Moreover, the dose to red bone marrow was estimated from the dose to the skeletal tissue taking into consideration the amount of active marrow in each irradiated bone [27]. Each run simulated the deposition of approximately 20 million photons originating from the X-ray source in order to allow the tally detectors to converge to a relative error smaller than 1%. Each simulation consumed approximately 30 min of computer time on a Pentium-IV class workstation.

Verification of the Monte Carlo dose calculations

An anthropomorphic phantom (Alderson Research Laboratories, Stamford, CT) and thermoluminescent dosimetry (TLD) were employed to verify computer simulation results. The Rando phantom, widely used to simulate the torso of an adult subject of 1.73 m height and 74 kg weight (BMI=24.7 kg/m^2), is cut into 36 transverse 2.5-cm-thick slices. Each slice contains cylindrical holes for the location of TLD material. Two hundred and forty lithium (TLD-100) and calcium fluoride (TLD-200) chips (Harshaw Co., OH) were utilized to monitor organ doses in the random phantom for every simulated projection. Two crystals were used in each position in the phantom. TLDs were calibrated by comparison with a 3-cm^3 Radcal (Radcal Corp., Monrovia, CA) ionization chamber. The chamber and the crystals were irradiated simultaneously in the same unit used for angioplasty interventions. The tube voltage was set at 75 kVp. TLDs were read using a Harshaw 3500 reader (Harshaw, Solon, OH). TLD crystals were aggregated into groups to achieve a standard deviation (SD) of the sensitivity factors less than 4% in each group. The background signal of all TLDs was measured, and the minimum detectable radiation dose for each group was determined as 2 SD of background signal. The phantom was loaded with TLDs at positions corresponding to the radiosensitive organ and tissues defined by the recommendations of ICRP [27, 28]. The phantom was exposed to separate fluoroscopy and DSA courses so that every projection was simulated according to the actual PTA procedure applied. Using the C-arm system involved in the patient study, the phantom was exposed to 250 Gycm^2 to reduce statistical errors in TLD signal measurements. The entrance skin dose was monitored by TLD-100 crystals attached on the phantom. The DAP-normalized dose to each organ or tissue in each slice of the Rando phantom was determined from the value of all TLDs using the equation:

$$D_{organ_i} = \frac{\sum_j f_{organ_j} d_{organ_{ij}}}{DAP} \quad (1)$$

where f_{organ_j} is the fraction of $organ_{ij}$ contained in Rando slice j, and $d_{organ_{ij}}$ is the dose to the fraction of $organ_i$ contained in phantom slice j [28]. All TLD crystals were measured immediately after irradiation.

Radiation risks

For the purpose of this study, the peak skin dose for typical procedures was compared to the thresholds for skin erythema and epilation, respectively [29]. Age- and gender-specific risks of carcinogenesis were quantified by multiplying the calculated effective dose with the risk of a cancer death attributable to uniform, whole-body, low-LET irradiation. Age- and sex-related fatal cancer risk factors (Table 1) were used [30].

Statistical analysis

Data statistical analysis was performed using MedCalc software (Medcal, Belgium). A Kolmogorov-Smirnoff test

Table 1 Age- and sex-related fatal cancer risks factors (NRPB 260 report)

Age at exposure (years)	Male	Female
10–19	9.0	10.9
20–29	6.1	7.0
30–39	4.3	4.6
40–49	4.2	4.2
50–59	4.2	3.8
60–69	3.3	2.9
70–79	1.7	1.6
80+	0.8	0.7
Average	5.8	5.9

confirmed that patient data followed a normal distribution. The significance level was set at $p=0.05$. All measured parameters were presented as mean values ± SD.

Results

Demographic data for study groups A and B are presented in Table 2. No statistically significant differences were observed between the two study groups. Stent placement was required in 70% and 86% for renal and iliac endovascular procedures, respectively. Parameters for fluoroscopy, digital radiography and angiography for renal and iliac procedures are presented in Table 3. The mean total fluoroscopy time and mean total DAP values for renal procedures were 16.9 min and 176 Gycm^2, respectively. For iliac procedures these values were 14.4 min and 127 Gycm^2, respectively.

The percentages of endovascular procedures in which CD was greater than the 2-Gy deterministic threshold for skin erythema were 2% and 7%, respectively. None of the treated individuals demonstrated deterministic skin responses of any kind. Moreover, the TLD estimated the PSD to a phantom-sized individual undergoing either a renal or an iliac PTA procedure, delivering DAP values to the patient equal to the mean. The DAP values reported in this study were lower than the 2-Gy threshold for deterministic effects.

Table 2 Demographic data of the two study groups A and B

	Group A (renal)	Group B (iliac)
Sex		
(Male:female)	18:6	51:5
Age range	42–76	50–85
Age (years)	63.2±10.5	66.7±8.9
BMI[a] (kg/m^2)	25.5±3.7	26.1±4.5
No stenting/stenting	7:17	8:48

[a]BMI: mody mass index

The total DAP to organ dose conversion coefficients derived from MC calculations for the PA, LAO 20° and RAO 20° projections used in renal and iliac endovascular procedures are presented in Tables 4 and 5 for 80 kVp and 5.5 mm Al/0.3 Cu filtration. Total DAP to effective dose conversion coefficients are presented in Table 6 for tube voltages ranging from 70 to 90 kVp and filtrations ranging from 5.5 mm Al/0.0 Cu to 5.5 mm Al/0.9 Cu. The effective dose per Gycm^2 varied from 103 to 371 μSv and 75 to 337 μSv for renal and iliac procedures, respectively. Comparison of MC calculated organ doses with values obtained from direct phantom measurements presented differences <15% for renal and <17% for iliac interventions, respectively.

In Fig. 1, age- and sex-specific radiation-induced cancer risks of patients undergoing renal and iliac PTA procedures are illustrated.

Discussion

Aortoiliac as well as renal artery PTA with or without stenting are common endovascular procedures performed routinely in most IR institutes [31, 32]. Endovascular therapy is the treatment of choice for TASC A and B lesions, while technical developments have led to increased initial success with endovascular treatments of even TASC C lesions. On the other hand, the high prevalence of RAS patients with coronary and lower extremity vascular disease has been well established [7, 33]. Fibromuscular dysplasia in young females and atherosclerosis in patients over the age of 55 are the most common causes. Endovascular treatment is nowadays the treatment of choice, and its clinical indications include poorly controlled hypertension refractory to medical therapy, worsening of renal function and flash pulmonary edema. Even when modern fluoroscopic equipment is used, renal or iliac endovascular procedures can still yield significant radiation doses to radiosensitive organs in the abdominal area and sometimes are associated with a risk of radiation injury [34].

Exposure parameters recorded for patients in the current study were in compliance with data reported from the RAD-IR study [6, 7]. Mean DAP and CD values reported by the RAD-IR study were slightly larger than those recorded in the present work. This may be attributed to the fact that a low-dose pulsed fluoroscopy unit was employed in our study. The iliac PTA/stenting procedure reported by the current study utilized a PA and an oblique projection, requiring an average of 80 and 20 percent of the procedure's fluoroscopic time, respectively. For this type of procedure the average DAP value was 127 Gycm^2, and the average effective dose to a male/female patient would

Table 3 Operating and radiation exposure parameters recorded for patients in study groups A and B involved in renal and iliac PTA procedures

	Group A (renal PTA) (Mean values ± SD)	Group B (iliac PTA) (Mean values ± SD)
kV(fluoroscopy)	76.6±7.6	73.7±6.8
mA(fluoroscopy)	28.2±15.4	34±8.1
SSD* (cm)	68±2	68±3
kV (DR*)	78.8±12.3	66.5±6.7
mAs (DR*)	54±15	58±19
# frames	150±108	152±126
# digital radiographs (DRs)	2±1.2	3±1.8
% use of oblique projections	12±10	20±10
Fluoroscopy time (min)	16.9±13.4	14.4±4.8
DAP-DSA* ($Gycm^2$)	162±45	114±48
DAP-fluoro* ($Gycm^2$)	11±7	9±8
Total-DAP ($Gycm^2$)	176±46	127±52
CD* (mGy)	1,193±547	990±392
% CD >1 Gy	23	21
% CD >2 Gy	7	2

*SSD: source-to-skin distance, DR: digital radiography, DAP: dose-area product, DSA: digital subtraction angiography, CD: cumulative dose

be approximately 17 mSv at 80 kVp/5.5 mm Al+ 0.3 mmCu. The corresponding effective dose value for a renal procedure would be approximately 42 mSv. McParland has reported an effective dose range of 1.3 to 39.1 mSv with a mean value of 13.6 mSv for a small sample of renal angioplasty procedures imparting 7.9 to 245 $Gycm^2$ to the patients [35]. Ruiz Cruces et al. reported a mean value of 61 $Gycm^2$ for abdominal angiography resulting in an effective dose of 0.8 mSv per minute of fluoroscopy [17]. However, these reports

Table 4 Organ (μGy) values normalized over the total dose-area product for projections involved in renal PTA procedures (per $Gycm^2$)

	PA	LAO-20°
Ovaries (female)	363	340
Testes (male)	4	5
Active bone marrow	372	356
Lungs	76	71
Colon	195	172
Kidneys	2,119	2,049
Adrenals	1,383	1,336
Stomach	437	374
Urinary bladder	51	45
Gall bladder	578	439
Spleen	1,142	851
Pancreas	701	690
Thymus	12	13
Breasts	13	12
Liver	574	564
Esophagus	42	39
Thyroid	1	1
Heart	75	67
Skeleton	405	412
Skin	132	143
Remainder	677	615

Tissues in bold characters represent organs for which the ICRP has assigned a weighting factor for the calculation of effective dose. Values smaller than 0.1 μGy were considered as zero. Tube voltage was set at 80 kVp/5.5 mmAl+0.3 mm Cu

Table 5 Organ (μGy) values normalized over total dose-area product for projections involved in iliac PTA procedures (per $Gycm^2$)

	PA	LAO-20°	RAO-20°
Ovaries (female)	604	570	514
Testes (male)	277	187	183
Active bone marrow	256	240	238
Lungs	1	1	1
Colon	561	608	411
Kidneys	18	16	17
Adrenals	3	2	2
Stomach	12	13	18
Urinary bladder	402	347	352
Gall bladder	26	22	28
Spleen	6	8	4
Pancreas	7	7	6
Thymus	0	0	0
Breasts	0	0	0
Liver	8	6	8
Esophagus	0	0	0
Thyroid	0	0	0
Heart	1	1	1
Skeleton	373	361	360
Skin	160	162	163
Remainder	97	86	92

Tissues in bold characters represent organs for which the ICRP has assigned a weighting factor for the calculation of effective dose. Values smaller than 0.1 μGy were considered as zero. Tube voltage was set at 80 kVp/5.5 mmAl+0.3 mm Cu

have utilized conversion coefficients for radiographic projections derived from the National Radiological Protection Board (NRPB) [36] that are rough approximations of the PTA employed projections. In the current study, an exact representation of the actual X-ray geometry was replicated for a renal or iliac endovascular procedure.

According to the findings of our study, organs that receive considerable amounts of radiation dose during iliac interventions are the gonads, the lower intestine and the

Table 6 Effective dose (μSv) values normalized over the total dose-area product for projections involved in renal PTA procedures (per $Gycm^2$) for various tube voltages and filtrations

		70 kVp, 5.5 mmAl				80 kVp, 5.5 mmAl				90 kVp, 5.5 mmAl			
Procedure	Filtration Cu (mm)	0.0	0.3	0.6	0.9	0.0	0.3	0.6	0.9	0.0	0.3	0.6	0.9
	Eff. dose												
Renal PA	Male	112	174	204	221	136	203	233	251	156	224	253	269
	Female	147	234	276	302	181	276	319	344	210	307	348	371
Renal LAO	Male	103	160	187	203	125	187	214	230	144	206	233	247
	Female	135	216	256	280	166	254	294	318	193	281	318	339
Iliac PA	Male	98	158	186	203	121	186	215	232	141	207	234	250
	Female	132	213	252	275	163	251	291	314	190	279	316	337
Iliac LAO	Male	87	141	168	184	108	168	196	212	127	188	215	230
	Female	128	208	246	268	158	245	283	306	185	272	310	330
Iliac RAO	Male	75	122	144	158	93	143	166	180	109	160	182	195
	Female	110	177	209	229	136	210	243	263	159	234	267	285

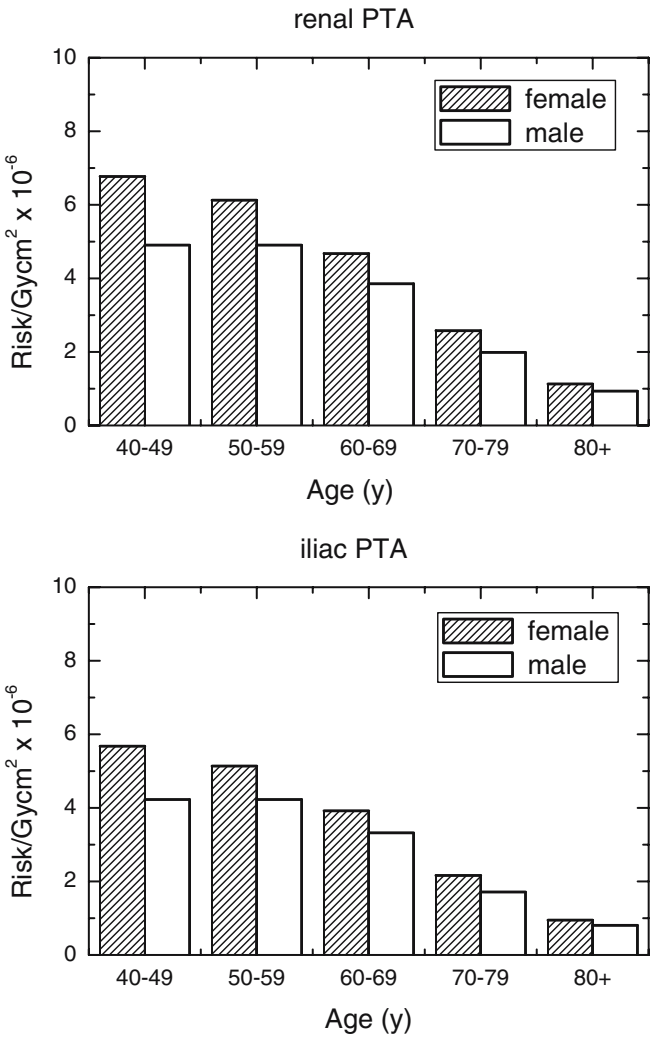

Fig. 1 Illustration of the dependence of radiation-induced cancer risk on the age and sex of an individual undergoing fluoroscopically guided PTA procedures. Risk estimations are shown for procedures involving iliac and renal angioplasty per Gycm^2 of the total procedure DAP

bladder. In renal interventions, the kidneys, the adrenals, the spleen, the liver and pancreas are the organs/tissues that are being irradiated. Differences between MC calculated normalized doses and normalized data obtained from direct TLD measurements were <15% for renal and <17% for iliac interventions, respectively. Individual organ dose differences in both cases may be attributed to differences between the location of organs in the Rando phantom and the setting of organs in the mathematical phantom adopted for our MC simulations. Additionally, inaccuracies in patient organ doses are also due to uncertainties associated with the use of TLDs. The overall uncertainty of TLD measurements was less than 15%.

A small percentage of procedures examined in this study demonstrated CDs higher than the 2-Gy threshold for the induction of a transient skin erythema, although no skin responses were recorded. The likelihood and severity of radiation-induced skin injury to the patient are a function of the PSD. However, depending on the patient's size, the table height and the angulation of the X-ray beam, the CD measurement point may be outside the patient, may coincide with the skin surface or may be inside the patient. Additionally, in case of beam angulations, the CD may deviate from the PSD due to the backscatter factor or attenuation of the beam in parts of the X-ray equipment. Therefore, the CD may overestimate or underestimate the PSD and should not be taken as a threshold for induction [7].

Compared with male individuals of the same age, female patients aged 40 to 49 years old are subjected to an increased fatal cancer risk compared to older subjects. Specifically, six and seven extra fatal malignancies are expected per Gycm^2 in excess to the naturally occurring ones for female patients between 40 and 49 years old undergoing iliac and renal PTA angioplasty. Risk estimates were calculated on the basis of risk coefficients derived from follow-up reports on atomic-bomb survivors, from animal studies and from patients who received non-malignant radiotherapy treatment. Therefore, considerable uncertainty exists concerning the risks associated with low-dose radiation.

However, patients treated with endovascular procedures may endure even higher radiation doses due to fluoroscopy of thick body masses, the short distance from the source to the entrance of the skin surface, multiple procedures, extended exposure times affected by the clinical condition of the patient and the level of experience of the interventional radiologist. Maximum DAP values reported from the RAD-IR study for PTA iliac and renal stenting procedures were 657 and 464 Gycm^2, respectively [6]. Consequently, special care must be taken when these procedures involve relatively young subjects. Although radiation risks cannot be neglected, the risks of not performing the procedure should also be taken into account.

Various uncertainties are associated with the determination of radiation doses and risk estimates presented in this study. Sources of error related to dose measurements include errors in TLD measurements and errors due to variations of the patient's size from the average. Variations in the position and size of organs in actual patients from the position and size assumed in our phantoms may contribute to the error in dose data estimation. However, the use of normalized doses utilizing mathematical phantoms instead of tailored individual calculations is currently the most realistic approach to the issue of effective dose estimation. Cancer risks presented in this study were obtained using risk coefficients derived from epidemiological data and based on the linear non-threshold dose-response models.

Therefore, uncertainties exist for risks associated with low-dose radiation.

Conclusion

In the current study, normalized radiation doses and risks are presented for typical fluoroscopically guided renal and iliac PTA/stenting procedures in the abdominal region. Most PTA/stenting procedures can result in considerable radiation doses to the patient, even when performed with modern fluoroscopic equipment. Even higher radiation doses can be imparted due to extended exposure times affected by the clinical condition of the patient and the level of experience of the interventional radiologist. Fatal cancer risks cannot be neglected, especially for relatively young individuals.

References

1. Spies JB, Bakal CW, Burke DR et al (2003) Angioplasty standard of practice. J Vasc Interv Radiol 14:S219–S221
2. Pentecost MJ, Criqui MH, Dorros et al (2003) Guidelines for peripheral percutaneous transluminal angioplasty of the abdominal aorta and lower extremity vessels. J Vasc Interv Radiol 14: S495–S515
3. Vorwerk D, Gunther RW (2001) Percutaneous interventions for treatment of iliac artery stenoses and occlusions. World J Surg 25:319–326
4. Olin JW (2004) Renal artery disease: Diagnosis and management. Mt Sinai J Med 71:73–85
5. Simon N, Franklin SS, Bleifer KH, Maxwell MH (1972) Clinical characteristics of renovascular hypertension. JAMA 220:1200–1218
6. Miller DL, Balter S, Cole PE et al (2003) Radiation doses in interventional radiology procedures: the RAD-IR study. Part I: overall measures of dose. J Vasc Interv Radiol 14:711–727
7. Miller DL, Balter S, Cole PE et al (2003) Radiation doses in interventional radiology procedures: the RAD-IR study. Part II: skin dose. J Vasc Interv Radiol 14:977–990
8. Vano E, Gonzalez L, Fernandez JM, Guibelalde E (1995) Patient dose values in interventional radiology. Br J Radiol 68:1215–1220
9. Marshall NW, Chapple CL, Kotre CJ (2000) Diagnostic reference levels in interventional radiology. Phys Med Biol 45:3833–3846
10. Perisinakis K, Raissaki M, Damilakis J, Stratakis J, Neratzoulakis J, Gourtsoyiannis N (2006) Fluoroscopy-controlled voiding cystourethrography in infants and children: are the radiation risks trivial? Eur Radiol 16(4):846–851, Apr
11. Imanishi Y, Fukui A, Niimi H et al (2005) Radiation-induced temporary hair loss as a radiation damage only occurring in patients who had the combination of MDCT and DSA. Eur Radiol 15(1):41–46, Jan
12. International Commission on Radiological Protection (2000) Avoidance of radiation injuries from medical interventional procedures. ICRP Publication 85. In: Ann ICRP 30, Pergamon Press, Oxford
13. European Commision (1999) Guidance on diagnostic reference levels for medical exposures. Radiation protection 109, Office for Official Publications of the European Communities, Luxembourg
14. Food and Drug Administration (1995) Recording information in the patient's medical record that identifies the potential for serious X-ray induced skin injuries. Center for Devices and Radiological Health, Rockville MD
15. McParland BJ (1998) Entrance skin dose estimates derived from dose-area product measurements in interventional radiological procedures. Br J Radiol 71:1288–1295
16. Ruiz Cruces R, Garcia-Granados J, Diaz Romero F, Hernandez Armas J (1998) Estimation of effective dose in some digital angiographic and interventional procedures. Br J Radiol 71:42–47
17. Gkanatsios NA, Huda, W, Peters KR (2002) Adult patient doses in interventional procedures. Med Phys 29:717–723
18. Struelens L, Vanhavere F, Bosmans H et al (2005) Effective dose in angiography and interventional radiology: Calculation of conversion coefficients for angiography of the lower limbs. Br J Radiol 78:135–142
19. Stratakis J, Damilakis J, Hatzidakis A et al (2006) Radiation dose and risk from fluoroscopically guided percutaneous biliary procedures. J Vasc Interv Radiol 17:77–84
20. Schultz F, Geleijns J, Spoelstra F, Zoetelief J (2003) Monte Carlo calculations for assessment of radiation dose to patients with congenital heart defects and to staff during cardiac catheterizations. Br J Radiol 76 (909):638–647
21. International Electro-Technical Commission (2000) Report 60601: medical electrical equipment-part 2–43: particular requirements for the safety of X-ray equipment for interventional procedures. IEC 60601-2-43, Geneva, Switzerland
22. Dormandy JA, Rutherford RB (2000) Management of peripheral arterial disease (PAD). TASC Working Group. TransAtlantic Inter-Society Concensus (TASC). J Vasc Surg. 31:S1–S296
23. Briesmeister J (ed) (2000) MCNP-a General Monte Carlo N-particle transport code, version 4C2. Los Alamos National Laboratory Report. LA-13709-M, Los Alamos, New Mexico
24. Eckerman K, Cristy M, Ryman J (1986) The ORNL mathematical phantom series. Oak Ridge National Laboratory (ORNL) Report. Available online at http://homer.hsr.ornl.gov/VLab/VLabPhan.html
25. Nowotny R, Hofer A (1985) A program for calculating diagnostic X-ray spectra. Rofo 142:685–689
26. International Commission on Radiological Protection (1990) Recommendations of the International Commission on Radiological Protection. ICRP Publication 60, In: Ann ICRP Vol 21, Oxford: Pergamon Press

27. International Commision on Radiological Protection (2002) Basic anatomical and physiological data for use in radiological protection: reference values (The International Commission on Radiological Protection, report of the task group on reference man) ICRP Publication 89, Ann ICRP 32, Elsevier Science Ltd, Oxford, UK
28. Perisinakis K, Theocharopoulos N, Karkavitsas N et al (2002) Patient effective radiation dose and associated risk from transmission scans using Gd-153 line sources in cardiac SPECT studies. Health Phys 83:66–74
29. Wagner LK (1995) Biological effects of high X-ray dose. In: Balter S, Shope T, eds, Syllabus: A Categorized Course in Physics. Oak Brook, III: Radiological Society of North America, pp 167–170
30. National Radiological Protection Board (1994) Estimates of radiation detriment in a UK population, NRPB-R260 National Radiological Protection Board, Didcot, UK
31. Tunis SR, Bass EB, Steinberg EP (1991) The use of angioplasty, bypass surgery and amputation in the management of peripheral vascular disease. N Eng J Med 325:556–562
32. Mackrell PJ, Langan EM 3rd, Sullivan TM et al (2003) Management of renal artery stenosis: effects of a shift from surgical to percutaneous therapy on indications and outcomes. Ann Vasc Surg 17:54–59
33. Khosla S et al (2003) Prevalence of renal artery stenosis requiring revascularization in patients initially referred for coronary angiography. Cathet Cardiovasc Interv 58:400–403
34. Koenig TR, Wolff D, Mettler FA et al (2001) Skin injuries from fluoroscopically guided procedures: Part 1, characteristics of radiation injury. Am J Roentgenol 177:3–11
35. McParland BJ (1998) A study of patient radiation doses in interventional radiological procedures. Br J Radiol. 71:175–185
36. Hart D, Jones G, Wall BF (1994) Estimation of effective dose in diagnostic radiology from entrance surface dose and dose-area product measurements. NRPB-R262, National Radiological Protection Board, Chilton, UK, pp 1–57